

MEAN WAKE OF SURFACE-MOUNTED FINITE-HEIGHT SQUARE PRISMS OF SMALL ASPECT RATIO

Barbara L. da Silva

Department of Mechanical Engineering
University of Saskatchewan
57 Campus Drive, Saskatoon, Saskatchewan,
S7N 5A9, Canada
barbara.silva@usask.ca

Dylan G. H. Hahn

Department of Mechanical Engineering
University of Saskatchewan
57 Campus Drive, Saskatoon, Saskatchewan,
S7N 5A9, Canada
dylan.hahn@usask.ca

David Sumner

Department of Mechanical Engineering
University of Saskatchewan
57 Campus Drive, Saskatoon, Saskatchewan,
S7N 5A9, Canada
david.sumner@usask.ca

Donald J. Bergstrom

Department of Mechanical Engineering
University of Saskatchewan
57 Campus Drive, Saskatoon, Saskatchewan,
S7N 5A9, Canada
don.bergstrom@usask.ca

ABSTRACT

The mean wake of surface-mounted finite-height square prisms, or blocks, with aspect ratios $AR = 0.5, 0.7$ and 1 was investigated in a low-speed wind tunnel. Velocity measurements were made using both a seven-hole probe and the particle image velocimetry technique. The Reynolds number based on the blocks' width D was $Re = 7.5 \times 10^4$, and two different incoming flow conditions with boundary layer thicknesses of $\delta/D = 0.6$ and 2.0 were considered. The mean wake behaviour changed with AR , and important trends were identified based on critical points in the symmetry plane. The mean streamwise vorticity distribution revealed different flow patterns in the wake, depending on both AR and δ/D . For $AR = 1$ and both boundary layers, the vorticity distribution is similar to that of prisms with $AR > 1$. For $AR = 0.7$, a transitional behaviour is observed, while for $AR = 0.5$ the wake shows an additional pair of streamwise vorticity regions. This pattern was found to be related to flow reattachment on the free end of the block, which becomes more symptomatic for a thicker boundary layer.

INTRODUCTION

Surface-mounted finite-height square prisms are commonly found in engineering applications, which motivates the study of the flow around this type of structure. The flow around these prisms is more complex than the one around two-dimensional or "infinite" square prisms, due to the three-dimensionality added by the surface-mounted finite-height square prism's free end and junction with the ground plane (Fig. 1). The aspect ratio AR of the prism, defined as the ratio between the prism height H and its width D , $AR = H/D$, is an important parameter in the analysis of the flow. However, most studies have been dedicated to prisms of high aspect ratio AR (e.g., Yauwenas et al., 2019). Despite their common applications such as in the study of flow around low-rise buildings and roughness elements, the flow around square prisms of very small aspect ratio ($AR < 1$) has not been as extensively studied.

The wake of this type of bluff body follows some of the same trends observed for surface-mounted finite-height square prisms below the critical $AR = 3.5 \sim 4.5$, such as having weaker vortex shedding and no base vortices (Unnikrishnan et al., 2017; Heng and Sumner, 2020). Unique features have, however, been identified in the literature for prisms of $AR < 1$, here referred to as blocks. Okamoto et al. (1995) reported a change in the flow behaviour for $AR \geq 0.7$ when compared with $AR = 0.5$, for which flow reattachment was observed. The nature of the flow structures around blocks has not been extensively explored, however, and contradictions exist in the literature about this type of flow. For example, periodic vortex shedding for blocks with $AR < 1$ was reported by some researchers (Calluaud et al., 2000), while others did not detect significant periodicity (da Silva et al., 2022).

Sumner et al. (2016) and da Silva et al. (2022) reported the existence of two pairs of streamwise vorticity regions in the mean wake of a block with $AR = 0.5$. The outer vorticity pair, located closer to the ground plane, has the same vorticity signs as the ones found for taller prisms. The inner vorticity pair has opposite signs of rotation compared with the outer pair, which is associated with the existence of two

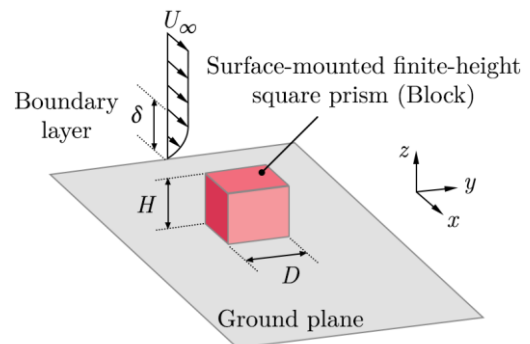


Figure 1. Schematic of the flow around a surface-mounted finite-height square prism of small aspect ratio (block).

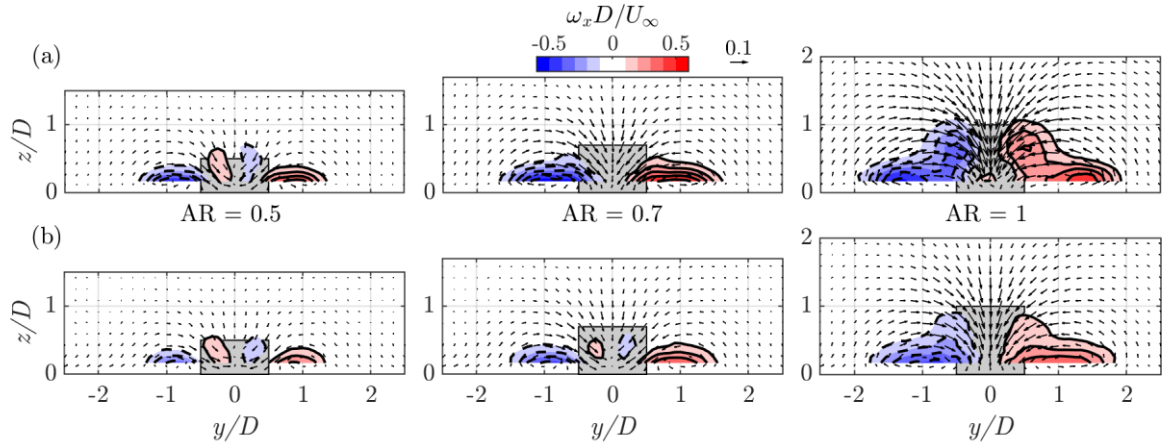


Figure 2. Mean streamwise vorticity distribution and in-plane velocity vectors (from the seven-hole pressure probe measurements) in a y - z plane located at $x/D = 3$ for surface-mounted blocks with $AR = 0.5$ (left), 0.7 (middle) and 1 (right). (a) Thin boundary layer with $\delta/D = 0.6$ and (b) thick boundary layer with $\delta/D = 2.0$. Every second vector in the y and z directions is shown, for clarity.

downwash peaks in the wake. This observation is in contrast to the single downwash peak found on the mean wake centreline for taller prisms.

The purpose of this study is to further investigate the mean wake of surface-mounted square blocks and the changes in the mean streamwise vorticity patterns by experimentally measuring the wakes of blocks with $AR = 0.5, 0.7$ and 1 . In addition, the effects of two different boundary layers with thicknesses of $\delta/D = 0.6$ and 2.0 will be assessed, as this parameter is expected to significantly affect the development of the wake (Heng and Sumner, 2020).

EXPERIMENTAL SET-UP

Experiments were performed using the low-speed wind tunnel of the University of Saskatchewan, with a set-up similar to that of Unnikrishnan et al. (2017) and da Silva et al. (2022). Hollow aluminum square blocks with sharp edges and black smooth surfaces were installed normal to the wind tunnel ground plane, with their front face normal to the incoming flow. The blocks had a constant width of $D = 60$ mm and aspect ratios of $AR = 0.5, 0.7$ and 1 .

The freestream velocity was $U_\infty = 21.1$ m/s, giving a Reynolds number of $Re = U_\infty D/\nu = 7.5 \times 10^4$ (where ν is the kinematic viscosity of the fluid). Two boundary layers were considered: a “thin” fully developed turbulent boundary layer of thickness $\delta/D = 0.6$, and a “thick” developing turbulent boundary layer with $\delta/D = 2$, produced by a trip near the leading edge of the ground plane. The corresponding boundary layer thicknesses relative to the blocks’ height (δ/H) vary from $\delta/H = 0.6$ for $AR = 1$ and the thin boundary layer to $\delta/H = 4.0$ for $AR = 0.5$ and the thick boundary layer.

Velocity measurements outside of the recirculation region of the wake were performed with a seven-hole pressure probe connected to a Scanivalve ZOC-17IP/8Px pressure scanner. By using a traversing system, the probe was positioned in y - z planes located at $x/D = 2$ (for $AR = 0.5$ only), 3 and 4 , where x is in the streamwise direction, y is in the transverse direction, z is normal to the ground plane, and the origin of the coordinate system is located at the centre of the junction of the block with the ground plane. Note that

measurements at $x/D = 2$ were not possible for $AR = 0.7$ and 1 due to reverse flow near the ground plane. Measurements in each plane were made for $y/D = -3$ to 3 and $z/D = 0.117$ to $AR + 1$, with intervals of 5 mm (or $0.083D$) between the points. Samples were taken during 10 s at a rate of 1 kHz. The uncertainty of the seven-hole probe measurements is less than 5% for the velocity magnitude and less than 3° for the flow angle.

Since the seven-hole probe is limited to a flow angle range of $\pm 72.9^\circ$, additional velocity field measurements were carried out with particle image velocimetry (PIV) in the x - z symmetry plane where reverse flow takes place. PIV measurements were carried out only for the thin boundary layer ($\delta/D = 0.6$). The flow was seeded by atomized propylene glycol droplets with diameters of less than $5 \mu\text{m}$. A 200-mJ/pulse dual Nd:YAG Solo PIV 200XT laser (New Wave Research) was used to illuminate the droplets in the flow field. Image pairs were obtained with a Powerview Plus 2MP camera (TSI), for fields of view of dimensions $0.91D \times 0.67D$, approximately. An ensemble of 2100 image pairs was sampled at a rate of 15 Hz for each field of view, and the Insight 3G software (TSI) was used for data acquisition and processing. The average uncertainty in the velocity measurements with PIV was evaluated as 4.5% .

RESULTS AND DISCUSSION

Results will be presented separately for the seven-hole probe and particle image velocimetry wake measurements.

Seven-Hole Probe Results

Figure 2 presents the mean streamwise vorticity ($\omega_x D/U_\infty$) in the y - z plane located at $x/D = 3$ for $AR = 0.5, 0.7$ and 1 , and for $\delta/D = 0.6$ (Fig. 2a) and 2.0 (Fig. 2b). Its distribution in the wake of the block of $AR = 1$ (the rightmost images in Fig. 2) follows the same pattern identified for surface-mounted finite-height square prisms below the critical AR by Unnikrishnan et al. (2017). The streamwise vorticity concentrations near the ground plane are either due to the trailing arms of the horseshoe vortex, or due

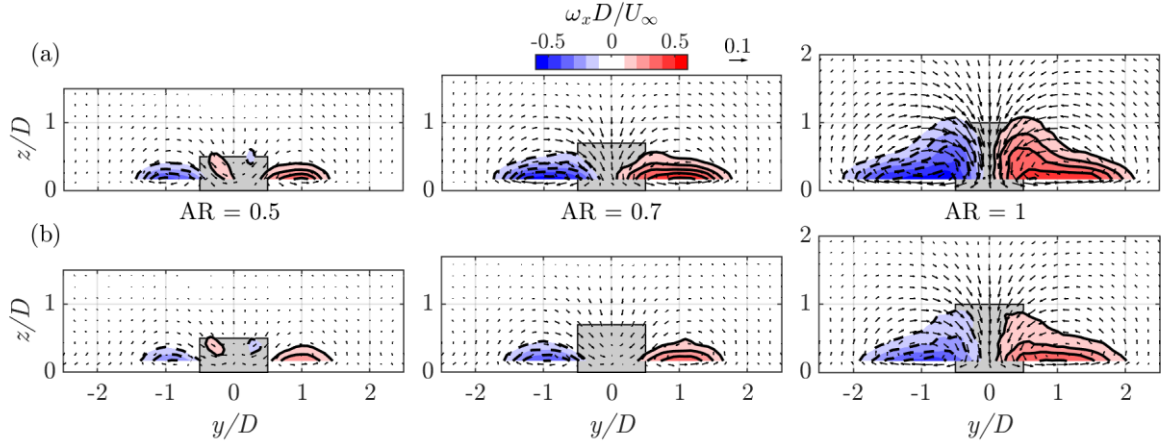


Figure 3. Mean streamwise vorticity distribution and in-plane velocity vectors (from the seven-hole pressure probe measurements) in a y - z plane located at $x/D = 4$ for surface-mounted blocks with $AR = 0.5$ (left), 0.7 (middle) and 1 (right). (a) Thin boundary layer with $\delta/D = 0.6$ and (b) thick boundary layer with $\delta/D = 2.0$. Every second vector in the y and z directions is shown, for clarity.

to an entrainment mechanism close to the ground plane (da Silva et al., 2022). These concentrations extend to the upper part of the wake. There, they are caused by the interaction of the free shear layers with the downwash, which is the strongest near the centre of the wake. By increasing the boundary layer thickness, the same pattern is found, but the downwash and the upper vorticity regions are weakened. In addition, some induced vorticity near the ground plane and the centre of the wake is found for $AR = 1$, with the thin boundary layer only.

The wake of the block with $AR = 0.5$ (the leftmost images in Fig. 2) presents the characteristics identified in Sumner et al. (2016) and da Silva et al. (2022). The outer vorticity regions near the ground plane, that were found for $AR = 1$ and reported in the literature for taller prisms, are still present. The downwash is, however, weaker in the centre. It shows instead two peaks (one at each y side of the wake) that are responsible for forming the inner vorticity regions with opposite signs of rotation, compared with the

upper streamwise vorticity that is typical in the wake of $AR = 1$ and taller prisms. The same pattern occurs for both boundary layers and with approximately the same vorticity intensity, although the thick boundary layer caused the inner vorticity regions to be flattened.

The mean streamwise vorticity in the wake of the block with $AR = 0.7$ (the central images in Fig. 2) shows distinct patterns for the two boundary layer thicknesses. With the thin boundary layer, neither the upper vorticity pair of $AR = 1$ or inner vorticity pair of $AR = 0.5$ is found. With the thick boundary layer, a small inner vorticity pair is present. This aspect ratio represents a transition state between the two mean vorticity patterns, where the upper vorticity has been weakened but the two downwash peaks are not yet strong enough to cause the appearance of the inner vorticity regions for the thin boundary layer case. By increasing the boundary layer thickness, the transition from the upper vorticity to the inner vorticity pattern is accelerated.

The streamwise evolution of the wake of the blocks can be analysed through the mean streamwise vorticity contours shown in Fig. 3 for the y - z plane located at $x/D = 4$. The wake has spread wider in the y direction for all cases, in agreement with Sumner et al. (2016). For $AR = 1$ (the rightmost images in Fig. 3), the upper vorticity regions have lower intensity, due to the weakened downwash at $x/D = 4$. The inner vorticity regions found for $AR = 0.5$ (the leftmost images in Fig. 3) have decreased in size for both boundary layers, while the inner vorticity pair found for $AR = 0.7$ and the thick boundary layer at $x/D = 3$ (centre of Fig. 2b) has disappeared at $x/D = 4$ (centre of Fig. 3b).

The behaviour presented in Fig. 3 indicates that the strength of the vorticity patterns – the typical upper vorticity or the inner vorticity pair with opposite senses of rotation – is related to the strength of the downwash, which decreases downstream in the wake. The mean streamwise vorticity distribution in the y - z plane with $x/D = 2$ shown in Fig. 4 for $AR = 0.5$ further confirms this observation. In this plane, the inner vorticity pair shows a large magnitude, especially in the lower part of the wake where the flow entrainment mechanism is more pronounced for this AR . The vorticity intensity is about the same with the thick boundary layer (Fig. 4b), but the size of the inner vorticity pair is reduced

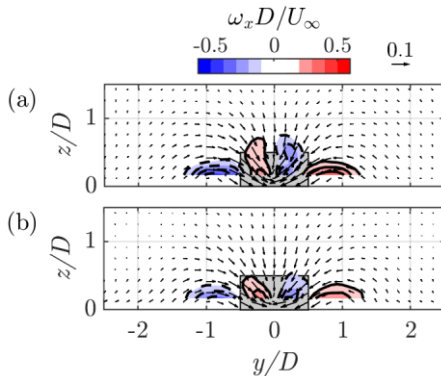


Figure 4. Mean streamwise vorticity distribution and in-plane velocity vectors (from the seven-hole pressure probe measurements) in a y - z plane located at $x/D = 2$ for the surface-mounted block with $AR = 0.5$. (a) Thin boundary layer with $\delta/D = 0.6$ and (b) thick boundary layer with $\delta/D = 2.0$. Every second vector in the y and z directions is shown, for clarity.

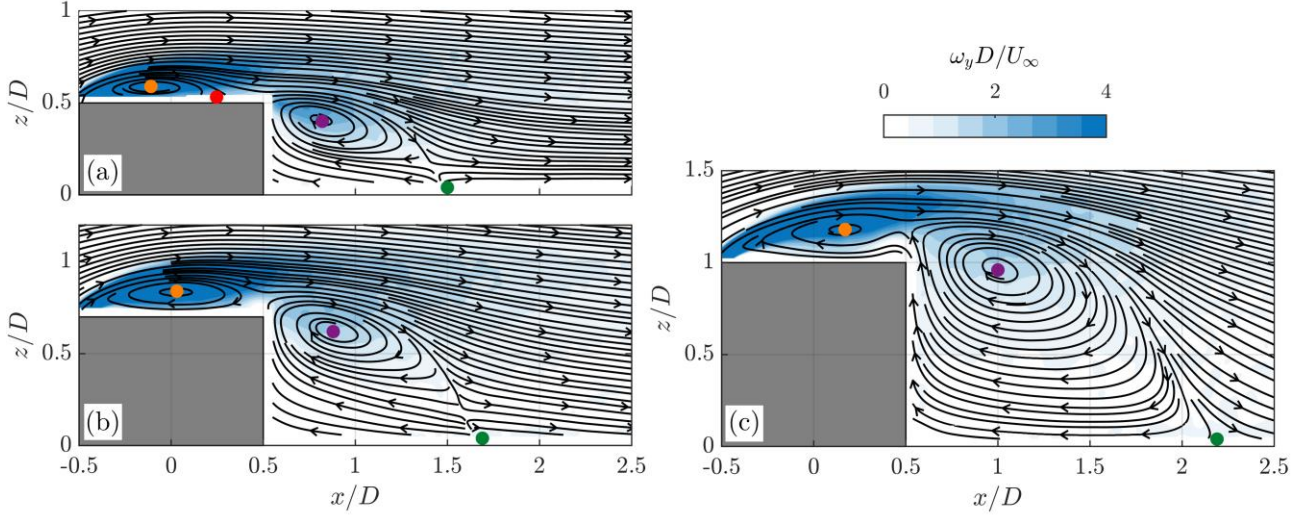


Figure 5. Mean transverse vorticity distribution and in-plane velocity streamlines (from PIV measurements) in the x - z symmetry plane ($y/D = 0$) for surface-mounted blocks with (a) $AR = 0.5$, (b) 0.7 and (c) 1 , and a thin boundary layer with $\delta/D = 0.6$. The orange, purple and green circles indicate the location of the free end vortex, vortex Bt and the approximate wake reattachment point, respectively. The red circle indicates the approximate reattachment point on the free end of the block with $AR = 0.5$.

Table 1. Main critical points in the x - z symmetry plane.

Critical point	$AR = 0.5$	$AR = 0.7$	$AR = 1$
Free end vortex centre	$x/D = -0.11$	$x/D = 0.03$	$x/D = 0.17$
	$z/D = 0.59$	$z/D = 0.84$	$z/D = 1.18$
Centre of vortex Bt	$x/D = 0.82$	$x/D = 0.88$	$x/D = 1.00$
	$z/D = 0.40$	$z/D = 0.62$	$z/D = 0.96$
Approx. wake reattachment point	$x/D = 1.50$	$x/D = 1.69$	$x/D = 2.19$

when compared with Fig. 4a. This behaviour is in agreement with the results obtained at $x/D = 3$ and 4 for $AR = 0.5$ (shown in Fig. 2 and 3).

Particle Image Velocimetry Results

Figure 5 presents the mean transverse vorticity component ($\omega_y D / U_\infty$) in the x - z symmetry plane of the wake of the blocks with $AR = 0.5$ (Fig. 5a), 0.7 (Fig. 5b) and 1 (Fig. 5c), for the thin boundary layer. The location of some of the main critical points in the wake are indicated by the coloured circles: the orange circle indicates the focus point corresponding to the centre of the free end vortex; the purple circle indicates the focus point corresponding to the centre of vortex Bt, following the nomenclature of Sumner et al. (2017) and Krajnović (2011); and the green circle indicates the approximate mean reattachment point of the wake. Note that the reattachment point is approximate as PIV measurements were carried out as close as 2 mm ($0.03D$) from the ground plane, to avoid excessive reflections. The locations of these points are presented in Table 1.

The wakes of all three blocks show common features to wakes of prisms below the critical aspect ratio, such as the absence of vortex Nw and the predominance of the large vortex Bt (Sumner et al., 2017). The location of the centre of vortex Bt moves closer to the block for smaller AR , but it

stays at approximately $z/H = 1$, moving slightly closer toward the ground plane for smaller AR .

The approximate wake reattachment point also corresponds to the maximum longitudinal length of the wake for the three aspect ratios. Table 1 and Figure 5 show that this length increases with AR , in contrast to the approximately constant maximum longitudinal length reported by Wang and Zhou (2009) for $AR = 1$ to 3 . This behaviour further suggests that different flow trends take place for the range of $AR \leq 1$, in comparison with other prisms below the critical AR .

The location of the free end vortex also changed significantly with AR . It moved upstream and downward for smaller AR , being located at $x/D < 0$ for $AR = 0.5$. Other notable flow features for $AR = 0.5$ are the two high-vorticity regions in the wake of this block, in Fig. 5a. The upper one is related to the shear layer that separated from the leading edge of the block, which is also observed for $AR = 0.7$ (Fig. 5b) and 1 (Fig. 5c). The lower region is found for $AR = 0.5$ only, originating due to the flow that has reattached on the block's free end subsequently separating from the trailing edge.

The red circle in Fig. 5a indicates the approximate reattachment point on the free end of the $AR = 0.5$ block, at $x/D = 0.25$. For the $AR = 0.7$ and 1 blocks, no reattachment was observed on the free end. This phenomenon is related not only to the smaller AR , but also to the higher probability of flow reattachment on the free end for larger boundary layer thickness relative to the prism's height (Castro and Robins, 1977). For the block with $AR = 0.5$ and the thin boundary layer, the boundary layer thickness relative to the block height is $\delta/H = 1.2$, meaning that this block is the only one of the three that is completely immersed in the boundary layer.

The present results suggest, therefore, that the occurrence of the inner vorticity pattern in the wake of the block with $AR = 0.5$ is connected to the reattachment of the flow over its free end. This observation is supported by the wake of the block with $AR = 0.7$ and the thick boundary layer ($\delta/H = 2.9$

versus $\delta/H = 0.9$ for the thin boundary layer), for which the inner vorticity pattern also occurred, at least at $x/D = 3$. However, since this pattern was not observed for $AR = 1$ and the thick boundary layer ($\delta/H = 2.0$), it is expected that reattachment on the free end of the block and the development of the inner vorticity pattern in the wake is not only a function of δ/H , but also of AR .

CONCLUSIONS

The mean wake of surface-mounted blocks was investigated for aspect ratios $AR = 0.5, 0.7$ and 1 , Reynolds number $Re = 7.5 \times 10^4$ and boundary layer thicknesses $\delta/D = 0.6$ and 2.0 .

Different mean flow patterns were identified in the wake of the blocks. For the boundary layer thickness with $\delta/D = 0.6$, a smaller aspect ratio was associated with a shorter longitudinal length of the wake and a free end vortex centre located closer to the leading edge of the block. The mean streamwise vorticity distribution had different patterns that were found to depend on both AR and δ/D . The upper vortex pair, typical of tall surface-mounted finite-height square prisms, was only found for $AR = 1$. It was weakened and replaced by an inner pair of vorticities with opposite sign of rotation for smaller AR and larger δ/D .

The occurrence of this inner vorticity pair appears to be related to flow reattachment on the free end of the block. These phenomena were found to be a function of both AR and δ/D (or δ/H), so further studies will be necessary to investigate in detail the relationship of the inner vorticity pair and flow reattachment on the free end with the flow parameters.

ACKNOWLEDGEMENTS

Financial support from the National Sciences and Engineering Research Council of Canada (Discovery Grants Program numbers RGPIN 05103-2016 and 2018-03760) and the University of Saskatchewan's Dean's Scholarship program is gratefully acknowledged. The technical support of S. Reinink, J. Bugg and Engineering Shops is also recognized.

REFERENCES

- Calluaud, D., David, L., and Texier, A., 2000, "Study of the laminar flow around a square cylinder", *Proceedings of the Ninth International Symposium on Flow Visualization*, Edinburgh, UK, Aug. 22–25, p. 402.
- Castro, I. P., and Robins, A. G., 1977, "The flow around a surface-mounted cube in uniform and turbulent streams", *Journal of Fluid Mechanics*, Vol. 79, pp. 307-335.
- da Silva, B. L., Sumner, D., and Bergstrom, D. J., 2022, "Mean and dynamic aspects of the wakes of a surface-mounted cube and block", *Journal of Fluids Engineering*, Vol. 144, p. 011302.
- Heng, H., and Sumner, D., 2020, "Wind loading of a finite prism: aspect ratio, incidence and boundary layer thickness effects", *Wind and Structures*, Vol. 31, pp. 255-267.
- Krajnović, S., 2011, "Flow around a tall finite cylinder explored by large eddy simulation", *Journal of Fluid Mechanics*, Vol. 676, pp. 294-317.
- Okamoto, S., Tsunoda, K., Takagi, T., Okada, E., and Kitani, K., 1995, "Near wake behind square cylinder of finite length on ground plane", *Transactions of the JSME Series B*, Vol. 61, pp. 3105-3113.
- Sumner, D., Unnikrishnan, S., Teng, M., Beitel, A., Das, A., and Fulton, M., 2016, "The mean wake of low-aspect-ratio surface-mounted finite-height square prisms and the effects of incidence angle", *Proceedings of the 8th International Colloquium on Bluff Body Aerodynamics and Applications*, Boston, MA, USA. June 7-11.
- Sumner, D., Rostamy, N., Bergstrom, D.J., and Bugg, J.D., 2017, "Influence of aspect ratio on the mean flow field of a surface-mounted finite-height square prism", *International Journal of Heat and Fluid Flow*, Vol. 65, pp. 1-20.
- Unnikrishnan, S., Ogunremi, A., and Sumner, D., 2017, "The effect of incidence angle on the mean wake of surface-mounted finite-height square prisms", *International Journal of Heat and Fluid Flow*, Vol. 66, pp. 137-156.
- Wang, H.F., and Zhou, Y., 2009, "The finite-length square cylinder near wake", *Journal of Fluid Mechanics*, Vol. 638, pp. 453-490.
- Yauwenas, Y., Porteous, R., Moreau, D. J., and Doolan, C. J., 2019, "The effect of aspect ratio on the wake structure of finite wall-mounted square cylinders", *Journal of Fluid Mechanics*, Vol. 875, pp. 929-960.